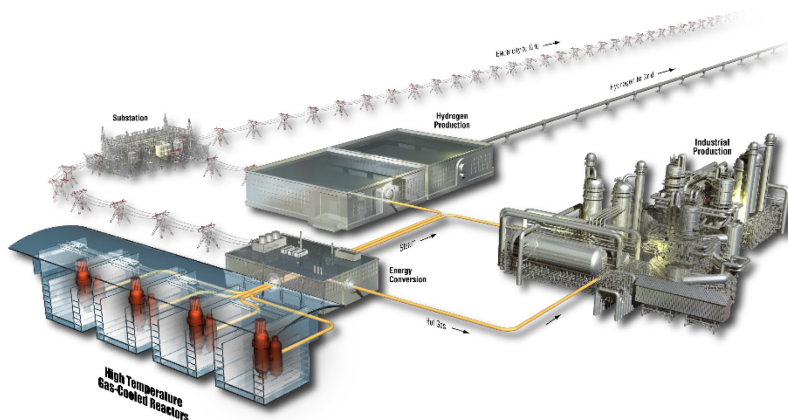


# Comparison of Oxidation Performance of Graphite Samples in TGA versus Vertical Furnace

Rebecca E. Smith

July 2019

The INL is a  
U.S. Department of Energy  
National Laboratory  
operated by  
Battelle Energy Alliance



#### **DISCLAIMER**

This information was prepared as an account of work sponsored by an agency of the U.S. Government. Neither the U.S. Government nor any agency thereof, nor any of their employees, makes any warranty, expressed or implied, or assumes any legal liability or responsibility for the accuracy, completeness, or usefulness, of any information, apparatus, product, or process disclosed, or represents that its use would not infringe privately owned rights. References herein to any specific commercial product, process, or service by trade name, trade mark, manufacturer, or otherwise, does not necessarily constitute or imply its endorsement, recommendation, or favoring by the U.S. Government or any agency thereof. The views and opinions of authors expressed herein do not necessarily state or reflect those of the U.S. Government or any agency thereof.

# **Comparison of Oxidation Performance of Graphite Samples in TGA versus Vertical Furnace**

**Rebecca E. Smith**

**July 2019**

**Idaho National Laboratory  
INL ART Program  
Idaho Falls, Idaho 83415**

**<http://www.inl.gov>**

**Prepared for the  
U.S. Department of Energy  
Office of Nuclear Energy  
Under DOE Idaho Operations Office  
Contract DE-AC07-05ID14517**



INL ART Program

Comparison of Oxidation Performance of Graphite  
Samples in TGA versus Vertical Furnace

INL/EXT-19-54584  
Revision 0

July 2019

Author:



Rebecca E. Smith  
Staff Engineer

7/10/2019

Date

**Technical Reviewer:** (Confirmation of mathematical accuracy, and correctness of data and appropriateness of assumptions.)




William E. Windes  
INL ART Graphite R&D Technical Lead

7/10/2019

Date

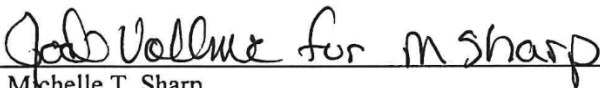
Approved by:



Gerhard Strydom  
Co-National Technical Director

7/10/2019

Date



Michelle T. Sharp  
INL Quality Assurance

7/11/2019

Date

## REVISION LOG

[illegible]



## SUMMARY

Data are presented to substantiate that comparison of rate data between TGA and vertical furnace results can be made for some well-defined conditions, but only in the context of consistent control. Substantial differences in sample dimensions and in geometric proportions can be somewhat compensated with mass normalization, as long as diffusion effects are small relative to the chemical kinetics (i.e., air flow is sufficiently high). Because variations in gas flow and variations in sample geometry can influence oxygen availability, presence of excess oxygen must be confirmed to validate the range of conditions over which the data from disparate systems can be compared. Statistical reproduction of testing over a suitable range of parameters appears to be more important than accommodating larger specimens, which necessarily limits the test matrix for irradiated materials.

In order to build a significant body of oxidation data from multiple research studies, all graphite oxidation testing must quantify the oxidation rate as a material-specific property by tightly controlling the test conditions so that intrinsic material-specific factors will govern the observed results. However, as this study demonstrates, graphite oxidation behavior is affected, to a greater or lesser extent, by a wide range of test-parameter variations other than just graphite grade and oxidation temperature. Additionally, practical constraints crucial for relating the observed oxidation of small test specimens to the oxidation behavior of larger, standardized test samples must be considered along with conditions keeping the tests focused on the intrinsic response. The major test parameters identified from this study are listed to highlight these experience derived insights into graphite oxidation testing.

1. Any oxidation test conducted outside the parameters established within a standardized test method (i.e., ASTM D7542) must be verified to supply excess oxygen (at the graphite surface) before the results can be compared to other oxidation results.
2. A test environment with surplus oxygen (an unvarying  $P_{O_2}^n$  term across the entire temperature range) completely surrounding the graphite test specimen is critical:
  - a. Before data from different oxidizing apparatus can be compared (i.e., vertical furnace versus TGA), the flow rate of the oxidizing gases must be established. Suitable gas flows—considering internal chamber diameter, specimen size, specimen geometry, and system capabilities—must be established to ensure surplus oxygen during testing.
  - b. For a direct comparison of TGA and vertical-furnace results (small specimens versus large specimen) excess oxidizing gas must be present for the full range of temperature test conditions. This will produce the same linear oxidation rate when averaged over the sample mass.
3. Theoretical graphite oxidation is traditionally conceived as three distinct temperature-dependent regimes. However, empirical rate data show a continuum response, where actual physical conditions at the extremes are theoretical approximations. A more meaningful model blends the characteristics of diffusion and chemical kinetics across the entire spectrum of observable performance.
  - a. From a practical perspective, low-temperature oxidation is very slow, and maintaining controlled experiment conditions for long periods is problematic. Also, at low temperatures, the anticipated flat concentration profile is still only approached for small and/or thin graphite specimens.
  - b. Alternately, high-temperature oxidation of small specimens is so rapid that the air-flow rate becomes reaction limiting, and real-time mass loss measurement becomes difficult.
4. While the observed oxidation response is a continuum, the **effect of oxidation** on the actual graphite material is dramatically different even across a limited span of experimental test temperatures (nominally 550 to 800°C):



- a. At high temperatures, graphite oxidizes only on the surface of the specimens and occurs as fast as oxygen can be transported to the surface of the sample; this is known as the “shrinking core” model of graphite oxidation. Little to no oxygen penetrates into the interior microstructure. *Because only the outer surface is affected, mechanical-strength loss is minimized at highest temperature when compared to low-temperature oxidation.*
  - b. At low temperatures, graphite oxidizes uniformly throughout the entire penetrated volume. The extent of oxidation in the sample interior will be nearly the same as the exterior surface. *Because of the internal damage, mechanical-strength loss is maximized when compared to high-temperature oxidation.*
  - c. All intermediate temperatures will produce a gradient of partial oxidation, with the penetration depth dependent upon the unique grade microstructure and test temperature.
5. Oxidation mass-loss progression falls into three distinct developmental periods:
    - a. *Onset*: The initial period is concomitant with the dynamic evolution of internal porosity. This is denoted as the non-linear, initial portion of the mass-loss to time curve before a stable rate of mass loss is achieved. It is conventionally defined as mass loss from 0–5%, and it can take up to 15% mass loss before the internal pore structure is fully established.
    - b. *Pseudo-steady-state*: This period corresponds to the stable relationship between gas gradients, graphite density gradient, and a consistent concentration of active sites (on average) sustained after onset. It is denoted as the nearly linear portion of the sigmoidal mass-loss-to-time curve. Conventionally, it is measured as mass loss from five to ten percent, but it more accurately occurs between 15 and 25% mass loss, after onset and before the pore microstructure is affected by significant mass loss.
    - c. *Tail*: The period at the end of oxidation, after significant mass loss has occurred, is when the asymptotic non-linear segment of the mass-loss curve reflects the approximate inverse of onset, where rate deceleration accompanies the declining concentration of active sites (on average across the sample, local porosity allows for ample gas exchange, but less and less graphite is locally present to react).
  6. Impurities within the (carbon) graphite material can significantly alter the oxidation rate and behavior. Contaminants may catalyze or inhibit oxidation (or neither), and the tail may exhibit the increasing influence of impurities as the ash residue represents progressively more of the remaining mass.
  7. Tests with fine-grain grades are more susceptible to an issue with small grains or particles separating from the surface of the specimen. This can produce artificially high measured oxidation rates.
  8. Sample size (fundamental differences in length scale) can produce notable variations, as exemplified by the variation in oxidation rate with extent of reaction. *Sample dimensions should be consistent to provide some control of onset variations.*
  9. The depth of oxidation penetration into the sample interior is interdependent to the density gradient caused by the progression of oxidative mass loss.
  10. Masking the contact surface of the sample from the impinging gas flow must be avoided. *The use of a closed bottom pan within a TGA system appears to influence the graphite-oxygen interface significantly.*
  11. Choose the correct normalization method for oxidation data.
    - a. For testing under ASTM D7542 that seeks to emphasize observable differences in performance among grades of graphite, surface area normalization is appropriate.

- b. However, in the interest of *comparing across different oxidizing systems*, specifically with varying length scales, mass-normalized data provide a more convenient tool for comparison.

These items summarize the observations that most impact oxidation behavior under experimental test conditions and provide the fundamental principles for comparison of test results from disparate experimental systems. Given the limited availability of irradiated graphite for oxidation test material, these principles are essential for developing meaningful experimental results relevant to nuclear reactor graphite applications



# CONTENTS

SUMMARY .....	vii
ACRONYMS.....	xiii
1. INTRODUCTION .....	1
1.1 Approach—Correlate Major Factors to Observed Variations in Oxidation Performance .....	1
1.2 Inherent Limitations.....	1
2. THEORY AND BACKGROUND .....	2
2.1 Oxidation Regimes.....	2
2.2 Oxidation Onset .....	4
2.3 Penetration Depth.....	6
2.4 Oxidizing Gas Exposure .....	7
2.4.1 Masking.....	8
2.4.2 Equivalent Sweep Velocity and Relative Sensitivity to Gas Flow Rate .....	8
2.5 Scoping Experiments on (TGA) Gas Flow (variations with NBG-25, NBG-18 and IG-110).....	9
2.5.1 Diminishing Influence of Increasing Flow .....	9
2.5.2 Naked Versus Pan Method.....	10
2.5.3 Sample Size and Fundamental Differences in Length Scale.....	11
3. MATERIALS AND METHODS .....	12
3.1 Basic Test Plan (and Its Basis).....	13
3.2 Selection of Sample Materials .....	14
3.3 ASTM Protocol as Adapted for Use .....	14
3.4 Normalization of Data.....	15
4. RESULTS AND ANALYSIS .....	17
5. CONCLUSIONS .....	19
6. REFERENCES .....	22

## FIGURES

Figure 1. Graphite oxidation model in three regimes with temperature dependence (top), oxygen concentration (middle), and density profile (bottom) with preferential attack of binder compared to filler.....	3
Figure 2. Typical progression of isothermal mass loss from virgin graphite to ash. ....	5
Figure 3. Cross-sectional perspective for cylindrical graphite samples (big and button) after immersion in air (for theoretical extremes and a conceptual hybrid). ....	7
Figure 4. Visible evidence of masking from basket-wire contact during isothermal oxidation at a nominal 750°C (left: NBG-18 after one percent mass loss in air, right: NBG-18 after one percent mass loss in ten percent air). ....	8
Figure 5. Effects of gas flow variations on NBG-25 oxidation in TGA (mass normalized oxidation rate).....	9
Figure 6. Sample geometry alters onset while approaching same linear oxidation rate. ....	11
Figure 7. Variations in onset for three TGA flow rates over the first 0.5% mass loss and up to 30% mass loss.....	13
Figure 8. NBG-25 graphite oxidation Arrhenius data: (a) surface area normalized and (b) volume normalized, and (c) mass normalized. ....	16
Figure 9. Self-consistent families of data for IG-110 (top) and for NBG-18 (bottom).....	17
Figure 10. Mass-normalized oxidation rates for IG-110 and NBG-18 in the TGA (buttons) and in the vertical furnace (buttons and big samples). ....	18

## TABLES

Table 1. Diminishing increases in oxidation rate (for NBG-25, in TGA pan, at 700°C) with incremental (30 mL/min) increases in air flow.....	10
Table 2. Naked IG-110 samples tested at 680°C to determine TGA air flow rate for oxidation testing. ....	12

## ACRONYMS

ART	Advanced Reactor Technologies
GC-MS	gas chromatography mass spectrometry
ICP-OES	inductively coupled plasma optical emission spectroscopy
TGA	thermogravimetric analyzer



# **Comparison of Oxidation Performance of Graphite Samples in TGA versus Vertical Furnace**

## **1. INTRODUCTION**

Oxidation influences the working life of nuclear graphite and can impact function during or after air (or steam) ingress accidents. Temperature, gas flow, oxygen content, and dimensional constraints at the microstructural and macrostructural levels can substantially influence the oxidation rate. The nature of these constraints must be considered when attempting to extrapolate performance from experimental results to service applications, but must also be evaluated in order to compare data among disparate experimental systems. This work compares oxidation test performance from a vertical furnace system (functioning as described by ASTM D7542) with tests using a thermogravimetric analyzer (TGA) adapted to operate in an analogous manner. From a few initial scoping studies, the hypothesis formed that, for a judiciously selected gas-flow rate, TGA performance would match the oxidation performance observed in the vertical furnace for the full range of graphite materials tested.

This report follows a conventional organization: introduction, theory, methods, results, and conclusions. The general approach is addressed first, then caveats. Next, basic principles are introduced, interrelated experimental observations are examined, and theoretic concepts are affirmed or refined. While the background includes considerable evidence from sometimes disparate prior test efforts, the resultant evaluation is shown to determine the parameters and controls inherent to this test plan. Ultimately, the collective details provide necessary context for the results and analysis enabling comparison of graphite oxidation performance in the TGA to those in the vertical furnace.

### **1.1 Approach—Correlate Major Factors to Observed Variations in Oxidation Performance**

Oxidation data from this study are offered to illustrate the major contributing factors in the observed variations in oxidation performance. Graphite oxidation testing under ASTM Standard D7542 is intended to quantify the oxidation rate as a material-specific property by tightly controlling the test conditions so that intrinsic material-specific factors will discernably influence the observed results. However, graphite oxidation behavior is affected, to a greater or lesser extent, by variations in test parameters as well. Absent an accepted true or inherent value for the observed (oxidative) mass loss rate, accuracy cannot be evaluated as such. The available body of data (range, average, and distribution of oxidation rate results) does allow for an assessment of the precision of this oxidation measurement technique. The accuracy of each system component is considered in this context, to assess potential configuration effects on performance. Practical constraints crucial for relating the observed oxidation of small test specimens to the oxidation behavior of larger items of graphite are examined along with evidence of their relative significance.

### **1.2 Inherent Limitations**

Many previous graphite oxidation studies present results that neglect to account for the (non-uniform) effects of oxidation (extent of reaction) on the oxidation rate. The rate accelerates, stabilizes, and then decelerates as any graphite specimen is progressively consumed from virgin material to ash. A crucial aspect of this study is the presentation of self-consistent results (specifically including traceable and consistent sample-source materials). The single greatest issue with comparison of oxidation data across different types of equipment or oxidation test methods is the difficulty in identifying and controlling all relevant variables. Analysis is further hindered by the labor-intensive nature of controlled oxidation testing: each point on an Arrhenius plot represents one or more days of equipment time and requires numerous experimental runs to acquire statistically meaningful data. The following discussion addresses all factors shown to have an observed influence on the oxidation rate.



## 2. THEORY AND BACKGROUND

Empirical data for small samples (of similar histories) generally support the exponential relationship between temperature and oxidation rate for conditions where the reaction is not oxygen limited. This relationship is described by the Arrhenius equation, commonly written as:

$$\text{rate} = k_0 e^{-\frac{E_A}{RT}} P_{O_2}^n \quad (1)$$

where  $k_0$  is the rate constant,  $E_A$  is the effective activation energy,  $R$  is the gas constant,  $T$  is temperature,  $P_{O_2}$  is the partial pressure of molecular oxygen, and  $n$  is the order of reaction.

One assumption is that for environmental conditions providing surplus oxygen (an unvarying  $P_{O_2}$  term across the entire temperature range), the log of the reaction rate varies linearly with the inverse of the temperature. This relationship is foundational for graphite oxidation experiments and for understanding the intrinsic kinetic behavior.<sup>1</sup>

### 2.1 Oxidation Regimes

Figure 1 shows a modified version of the classic figure from Walker et al.<sup>2</sup> Figure 1 illustrates the theoretical oxidation behavior with changing temperature over three regimes, offering a conceptual representation of the extremes of mass transport and chemical-reaction kinetics and the transition between them. In this context, the linearity of a consistently acquired Arrhenius data set can be assessed numerically with the Pearson correlation coefficient. Due to the inherent open porosity of nuclear graphite, the reactant (oxygen) can penetrate into the interior graphitic microstructure. Intuitively, the larger the temperature range observed, the less linear the overall correlation between the log of the oxidation rate and the inverse of the temperature appears. Conceived as three distinct regimes as indicated in Figure 1, the empirical rate data show a continuum where actual physical conditions at the extremes are theoretical approximations. A more meaningful model blends the characteristics of diffusion and chemical kinetics across the entire spectrum of observable performance.

Observation of the oxidation behavior across the full range of theoretical performance is hampered by several practical issues. Low-temperature oxidation is very slow, and maintaining controlled experimental conditions for the long periods necessary for suitable mass loss to occur is cumbersome. Also, at low temperatures where oxidation is still measurable, the anticipated flat concentration profile is still only approached for relatively small (thin) graphite specimens. Alternately, at the high-temperature extreme, such small specimens oxidize so rapidly that the air-flow rate becomes reaction limiting, and real-time mass loss measurement becomes difficult.

The binder material in graphite often appears to be more susceptible to oxidation than the filler material (individual grains): intact particles sometimes drop off the surface of a sample when more vulnerable surrounding material (presumed to be binder) has been corroded away. Conventional analysis from ASTM Standard D7542 employs the gross mass loss over time (i.e., average observed performance) for each given sample as an indication of reaction rate. However, clearly local oxidation rates vary significantly even within a sample of modest size. The three-regime model does not account for variations in performance between the binder and filler of any given graphite; it predicts only the average overall behavior of the bulk material. From direct experimental observations, large-grained materials seem to have an advantage (particularly at the high-temperature end of Regime 2) because grains at the sample surface are retained longer as internal porosity develops within the graphite. Small grains or particles incumbent to fine-grained graphite tend to separate from the surface of the specimen more readily (i.e., after less overall mass loss, and generally more quickly) than larger ones.

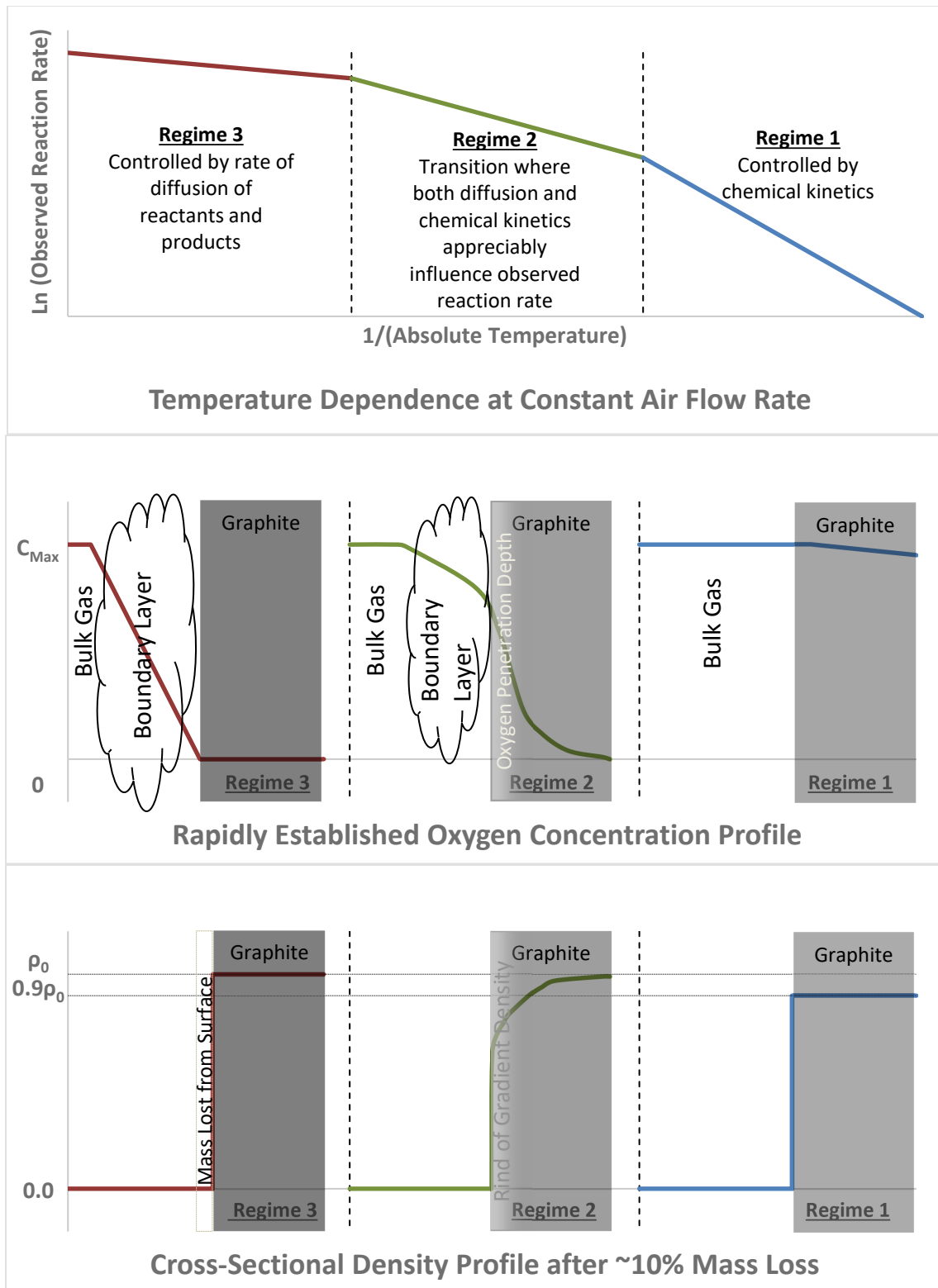


Figure 1. Graphite oxidation model in three regimes with temperature dependence (top), oxygen concentration (middle), and density profile (bottom) with preferential attack of binder compared to filler.

There has long been speculation that the kind of porous (presumably binder-depleted) surface material may provide a partial diffusion barrier, protecting the material interior, whereby the loss of particles from the sample surface artificially inflates the observed reaction rate (measured by mass loss) and exposes comparatively fresh reactive surface (phenomena parallel to the formation and sloughing of an oxide film on a metal surface). However, release of individual grains and any corresponding localized onset rate change can equally be explained by the evolving concentration of active sites within the graphite sample volume. Because both binder and filler are graphitic (and therefore the same at the crystallographic and chemical bonding level, unlike the oxide film on metal) the apparent binder-filler oxidation disparity is moot. However, the logic does offer a plausible intuitive explanation for the case when the incomplete oxidation associated with gross grain loss presents as a rapid and discontinuous observed rate.

At the bottom of Figure 1, the gray-scale gradient of the graphite adjacent to the boundary layer for Regime 2 is intended to illustrate this graded depletion of surface material from a monolithic graphite slab. The model for Regime 3 anticipates a “shrinking core” of graphite, where the reaction occurs entirely at the graphite surface with little to no penetration into the interior microstructure. The graphite body remains at nearly the same initial density, visually signified by the uniformly darker color in the figure. Conversely Regime 1 oxidation produces nearly uniform depletion of material throughout the graphite body and is understood to influence the binder nearly proportionately through the material thickness, as illustrated by the uniformly lighter color.

The rate dependence on extent of reaction (as measured by mass loss) poses yet another constraint as the nearly linear post-onset period tapers off at high mass loss with diminishing graphite sample mass. In cases where entire grains of sample begin to drop away (at the high temperatures of Regime 2) inconsistencies in mass-loss measurements may be amplified. There is simultaneously less precision in mass-loss measurement and a shorter time period for the measurement of relevant data.

## 2.2 Oxidation Onset

During oxidation testing, the rate of oxidation is observed to increase over an initial period before the rate stabilizes. (Usually these tests terminate before the oxidation rate tapers off.) By convention, the first five percent of mass loss is allowed for oxidation “onset” while the average oxidation rate from five to ten percent of mass loss is used to analyze the Arrhenius parameters (*Equation 1*). This onset assumption provides for a more robust assumption of similarity in sample history for virgin material, where for example, proximity to billet exterior after the final stage of graphitization could produce disproportionate variations in apparent onset. This simplifies analysis from these standardized tests by addressing the rate dependence on extent of reaction similarly across all test specimens, regardless of origin. However, the practice takes an extremely conservative notion of oxidation performance and completely discounts variations in onset.

This oxidation-behavior progression, concomitant with the dynamic evolution of internal porosity, is illustrated with a simple plot of sample mass loss versus time, as shown in Figure 2. Note that the generic symmetrical sigmoidal curve shown does not achieve linear oxidation before five percent mass loss is achieved, it only approaches the linear portion of the curve after approximately 12–15% mass loss. This experimental observation is consistent for both the NBG-18 and IG-110 samples tested. The actual form of the curve may also be noticeably asymmetrical due to contaminant materials found within all nuclear graphite grades. As the sample oxidizes to ash, the effect of impurities within graphite may have an increasing influence on the oxidation rate (as suggested by differences in curve shapes for the NBG-18 and IG-110 button results). Elemental data from aggregated gas chromatography mass spectrometry (GC-MS) and inductively coupled plasma optical emission spectroscopy (ICP-OES) test results measure an IG-110 nominal impurity of 20 ppm by weight, as compared to 70 ppm in NBG-18, nearly four times larger than IG-110.

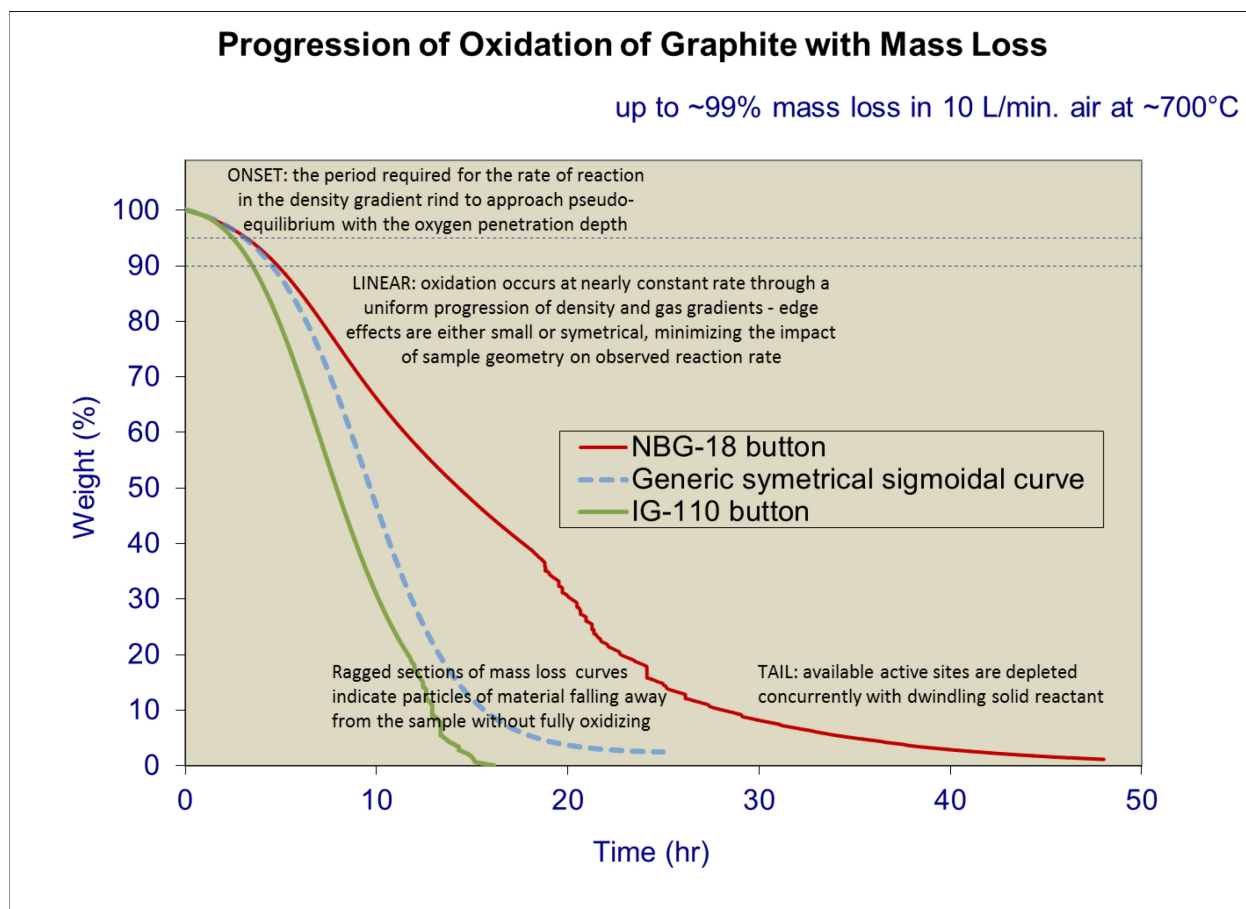


Figure 2. Typical progression of isothermal mass loss from virgin graphite to ash.

Oxidation onset reflects the period of rapidly changing oxidation rate not easily characterized by an average numeric rate value. By contrast, the five to ten percent mass loss period is relatively linear for all nuclear graphite grades and gives a fairly consistent (reproducible) rate value. Strength properties of graphite deteriorate precipitously beyond 15% mass loss for convenient sample sizes,<sup>3</sup> so attention has generally focused on the earlier portion of this period of linear mass loss. The transient onset period is systematically neglected, and the transient tail of the mass-loss curve, where the rate tapers off, remains outside the scope of investigation. This tail is not significant to the monolithic slab illustrated in Figure 1, but must be considered in the context of sample geometry in order to validate analytical assumptions necessary to evaluate chemical kinetics for a graphite material.

Employing consistent sample dimensions is a primary assumption for ASTM D7542 and does provide some control of onset variations. However, the shape of the mass-loss curve, including the nature and timing of inflections, is heavily dependent on the individual sample microstructure including both the presence of contaminants and the extent of graphitization. Onset appears to occur as a result of the early cascading increase in active oxidation sites within the graphite crystal structure. The linear rate (conventionally assumed to begin at five percent mass loss) corresponds to a stable relationship between the gas gradients, graphite density gradient, and a consistent concentration of active sites (on average) sustained after onset. The expansive generation of active sites during onset is mitigated by both local gas concentrations and the destruction of active sites: as these local mechanisms stabilize, the observed reaction rate becomes linear (to a good approximation), producing a pseudo steady-state oxidation rate. The non-linear variation in oxidation rate over the first few percent mass loss with the transition to the nearly linear rate of oxidation during the five to ten percent mass loss are surprisingly similar for high-

purity nuclear grades of graphite. Note, however, that a smaller interval will appear to be nearly linear (Pearson correlation  $0.98 < R^2 < 1.00$ ) almost anywhere along the plot of mass loss versus exposure time (apart from ragged sections where grain/particle loss presents discontinuities in the data). The convention of using the five to ten percent mass-loss range matches the standard practice described in ASTM D7542, neglecting the transitional rate observed in the onset period (arbitrarily defined as the approach to five percent mass loss).

When gross grain/particle loss is observed, it appears to be the culmination of a fully developed oxidation front. For a sufficiently large sample oxidizing within Regimes 1 and 2, some density gradient should propagate along with the oxygen gradient. This shift in the density gradient will occur with the loss of external grains over time until the sample exterior becomes completely depleted, and the residual surface material falls away (oxidizes or physically separates from the surface). Compared to experimentally-measured mass loss, oxygen penetration within the graphite microstructure is nearly immediate.<sup>4</sup> However, the period of onset needed for the reaction rates to produce the pseudo-equilibrium of active sites to approach the near-linear reaction rate (even with the ample excess of available oxygen) remains non-trivial for the estimation of kinetic parameters.

## 2.3 Penetration Depth

Oxygen penetration is interdependent, if not entirely causal, to any density gradient in the graphite that may become evident with the progression of oxidative mass loss. Local gas-concentration gradients in the boundary layer at and beneath the surface of the oxidizing graphite develop relatively rapidly and, therefore, do not fully explain the prolonged nonlinear onset phenomenon. Mass-loss trends for a specimen isothermally oxidized to five percent, cooled in inert gas, stored for a period, and later isothermally oxidized for another five percent mass loss can be stitched together to demonstrate a very good match for a specimen from the same graphite source oxidized to ten percent mass loss without interruption.

The qualitative trend in post-oxidation observations after one-, five-, and ten-percent mass-loss experiments, and the gradual development of the density gradient, make a general correlation with the gradual onset tempting. While a theoretical uniformity of graphite density would be expected at both extremes (Regime 1 and Regime 3), a nonlinear onset period seems to be in evidence across the full range of conditions and materials experimentally tested (conceptually consistent with only Regime 2 behavior). The bottom of Figure 1 indicates theoretical performance across an exposed surface of a graphite slab where height and depth are large, such that the cross section is not influenced by end effects. By contrast, the dimensional geometry effects are inherent to Figure 2 and are visualized for cross sections of nominal sample geometries as shown in Figure 3.

Direct comparison of TGA and vertical furnace results requires a combination of excess oxidizing gas for the full range of temperature test conditions producing the same nearly linear oxidation rate when averaged over the sample mass. In small samples suitable for testing within a TGA, at ten percent mass loss and at low to moderate temperatures, the gradient in density may be negligible. Presumably oxygen fully penetrates the small graphite sample and any edge effects (accelerated oxidation at surfaces and corners) would be minimal as the overall reaction rate is derived from the mass loss observed for the entire sample. Reduction in sample dimensions from oxidation at the sample surface would also be negligible, less than the error in measurement. Larger samples oxidized at higher temperatures are much more susceptible to these penetration-depth issues because their surfaces are disproportionately changed when compared to small samples. This problem can also cause considerable post-oxidation dimensional measurement error (additional release of particles from corroded surfaces with handling) depending upon oxidation conditions.

While the gas gradient appears to be established rapidly (in seconds or less for most test conditions), there are likely material-specific variations that evolve during onset, remain stable during the linear mass-loss period, and evolve further at the tail (approaching the end of oxidation) as the reacting material is

depleted. The oxygen gradient may be more dependent on temperature than on microstructure, particularly above  $\sim 800^{\circ}\text{C}$ . The density gradient, once established, should propagate uniformly during the linear mass loss period. The inherent assumption that the graphite reaction rate is linear over the five to ten percent mass-loss period is customarily validated with the Pearson correlation coefficient, where the expectation is that  $0.98 < R^2 < 1.00$ .

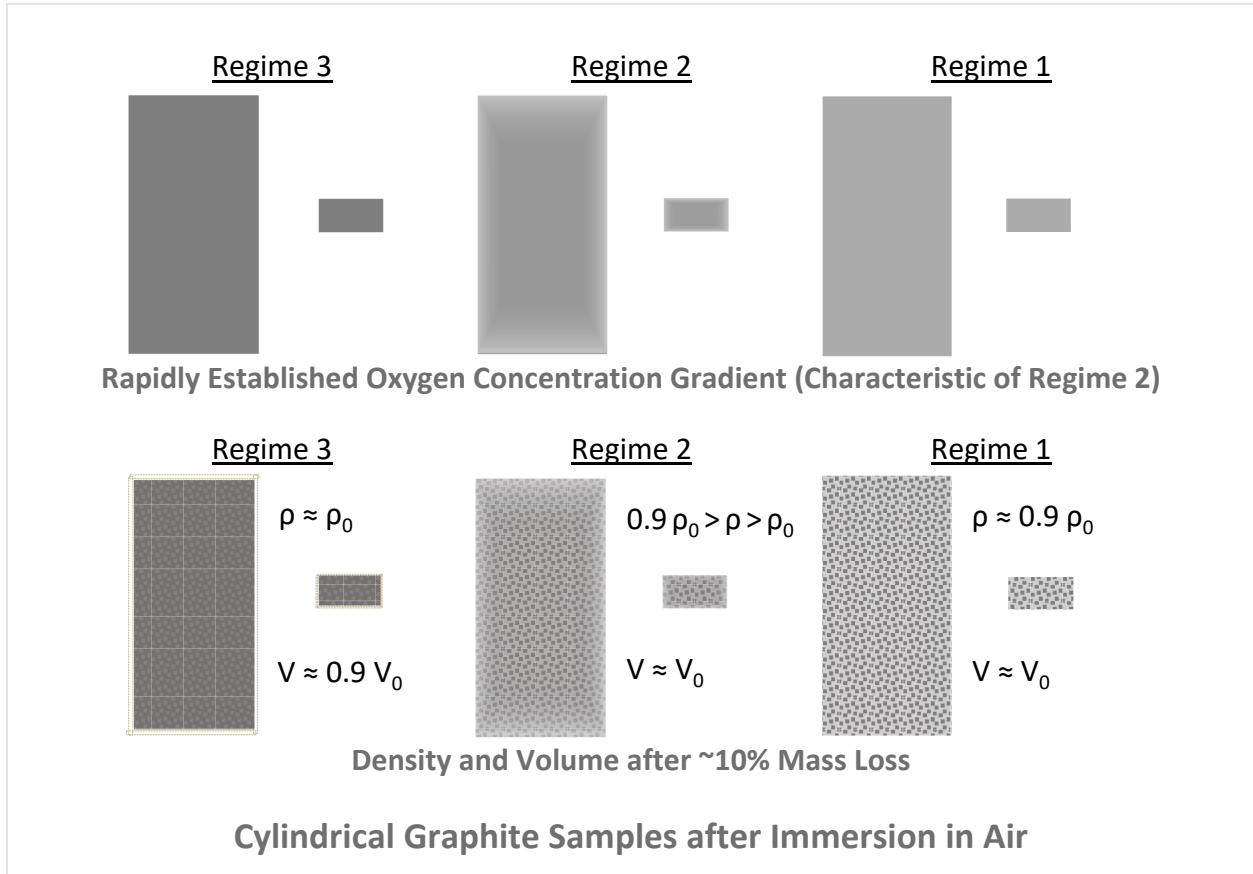


Figure 3. Cross-sectional perspective for cylindrical graphite samples (big and button) after immersion in air (for theoretical extremes and a conceptual hybrid).

## 2.4 Oxidizing Gas Exposure

Oxidizing gas exposure needs to be considered from three different perspectives to establish a uniform partial pressure of oxygen ( $P_{O_2}$  in *Equation 1*) and excess oxygen supply for the full range of test conditions: sample geometry (size and penetration-depth issues introduced above), inlet gas flow (flow rate and composition), and exposure to (or deflection of) the impinging flow (masking). ASTM D7542 provides guidance for gas-flow test parameters for the larger vertical furnace,<sup>5</sup> but the recommended 10 L/min gas flow exceeds the capacity for a normal TGA. The initial use of 30 mL/min flow was a practice carried over from a previous (unrelated) TGA experiment. This gas flow produced inadequate results for the much smaller sample size and internal volume of the TGA. The gas-flow rate parameter has subsequently been reconsidered to fit the purpose of the graphite oxidation work using specific assumptions from the development of ASTM D7542.

During the development of the standard, the gas flow rate was gradually increased over a controlled series of runs in a vertical furnace configuration. The observed oxidation rate increased with each increase in gas flow rate, with 10 L/min being the maximum rate tested due to limitations of the available

equipment. At 10 L/min, the resultant effect seemed to be diminishing, consistent with the principle that providing sufficient excess of oxidant prevents oxygen depletion in the environment from limiting the rate of oxidation and making further excess of minimal impact.

### 2.4.1 Masking

During previous vertical furnace testing, several samples recovered after one percent mass loss at temperatures above 700°C showed a surface pattern indicating that the basket wire masked the contact surface of the sample from the impinging gas flow, as can be seen in Figure 4. Oxidation tests at lower temperatures did not show visible evidence of this masking effect, supporting the principle that the reaction rate is less dependent upon diffusion at lower temperatures. By five percent mass loss, localized masking from the thin basket wire is usually obscured by the progression of oxidation along the concentration gradient within the surface microstructure.

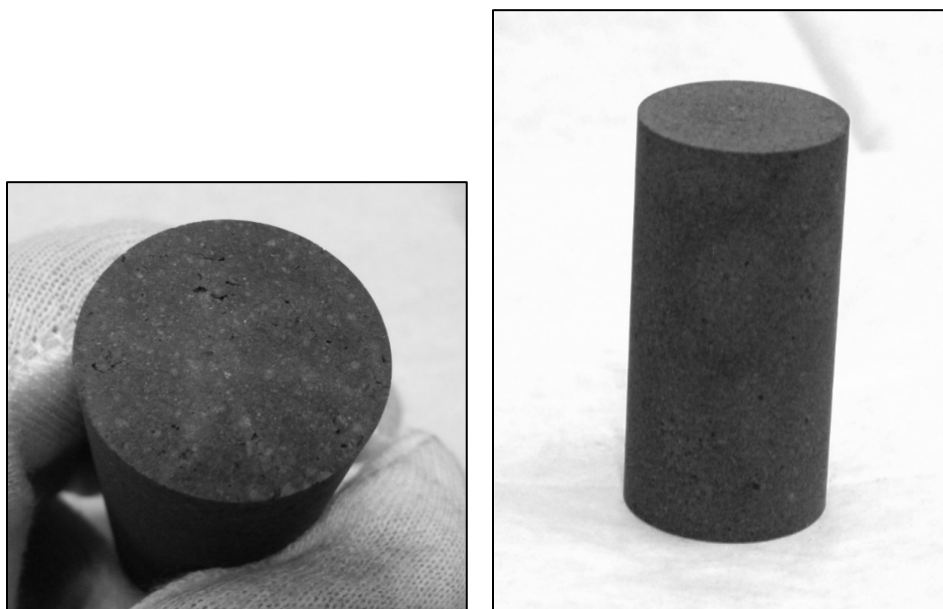


Figure 4. Visible evidence of masking from basket-wire contact during isothermal oxidation at a nominal 750°C (left: NBG-18 after one percent mass loss in air, right: NBG-18 after one percent mass loss in ten percent air).

### 2.4.2 Equivalent Sweep Velocity and Relative Sensitivity to Gas Flow Rate

The flow rate in the vertical furnace has been established as 10 L/min (10,000 mL/min) to be consistent with the standard conditions prescribed in ASTM D7254. The inside diameter of the vertical furnace tube is 6.35 cm (2.5 inches), with an intended nominal sample diameter of 2.54 cm (1 inch), giving a linear flow rate of 94 cm/min. A proportionate sweep velocity in the TGA, with its internal chamber diameter of 4 cm (1.57 inches) and nominal button-sample diameter of 1.27 cm (0.5 inch) would require a flow rate of 4.26 L/min, (4,260 mL/min) far beyond the functional range for this TGA instrument.

Given the recommended operating practices for the TGA, the effort to resolve an appropriate test parameter for TGA gas flow was approached in a manner similar to that employed for the establishment of the 10 L/min flow rate employed for the vertical furnace: a series of scoping tests were performed in an effort to find a set point that supports the diminishing influence of (further) increase in flow rate.

## 2.5 Scoping Experiments on (TGA) Gas Flow (variations with NBG-25, NBG-18 and IG-110)

A scoping experiment was carried out using NBG-25 buttons as indicated in Figure 5. Large samples of NBG-25 tested in the vertical furnace at a nominal oxidation temperature of 740°C showed oxidation performance indicative of diffusion effects—accelerated and choppy (nonlinear) mass loss due to release of grains/particles from the surface before ten percent of the initial sample mass was oxidized away. Therefore, the first several TGA samples were tested at a nominal 700°C oxidation temperature to avoid test conditions expected to produce similarly inconsistent results. These early TGA samples were suspended in the closed bottom “basket,” or pan, conventionally used with this particular instrument.

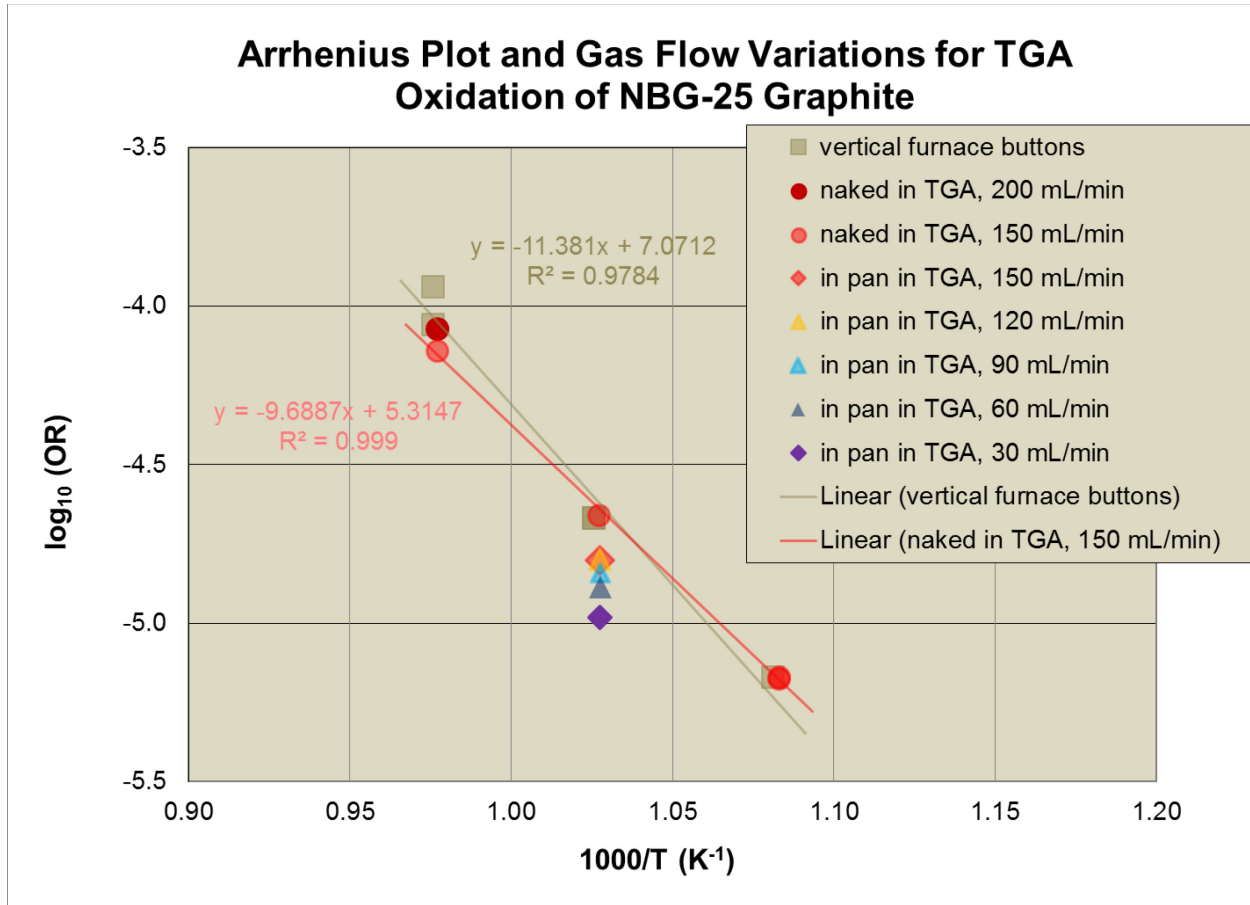


Figure 5. Effects of gas flow variations on NBG-25 oxidation in TGA (mass normalized oxidation rate).

### 2.5.1 Diminishing Influence of Increasing Flow

Incrementally increasing the gas flow rate set point from 30 to 150 mL/min over a series of five otherwise equivalent NBG-25 test runs in the TGA produced clear, corresponding increases in the observed reaction rate. The higher the flow, the smaller the observed increase in rate, as indicated in Table 1. There was no evidence of a choppy, nonlinear mass loss or wholesale release of particles. However, the closed bottom of the pan would have retained any such material released from the sample surfaces regardless, and the pan may also have masked the contacting surface of the graphite button or otherwise deflected the flow of oxidizing gas around the button sample. By comparison to the other 30 mL/min step increases in the oxidizing gas flow, the increase from 120 to 150 mL/min produced a much smaller change in the observed oxidation rate.



Table 1. Diminishing increases in oxidation rate (for NBG-25, in TGA pan, at 700°C) with incremental (30 mL/min) increases in air flow.

Air Flow Rate (mL/min)	Surface Area Normalized Oxidation Rate ( $\text{g h}^{-1} \text{m}^{-2}$ )	Change in Oxidation Rate ( $\text{g h}^{-1} \text{m}^{-2}$ )	Mass Normalized Oxidation Rate ( $\text{g s}^{-1} \text{g}_0^{-1}$ )	Change in Oxidation Rate ( $\text{g s}^{-1} \text{g}_0^{-1}$ )
30	105.9	—	1.0431E-05	—
+30	—	+27.27	—	+2.543E-06
60	133.17	—	1.2975E-05	—
+30	—	+13.43	—	+1.381E-06
90	146.6	—	1.4356E-05	—
+30	—	+14.28	—	+1.545E-06
120	160.88	—	1.5901E-05	—
+30	—	+0.47	—	-6.192E-08
150	161.35	—	1.5839E-05	—

## 2.5.2 Naked Versus Pan Method

Given the masking effects observed in vertical furnace experiments, the exposure to the impinging flow of the oxidizing gas seemed likely to be influenced by the extent of deflection around the suspension construct as well as the inlet gas flow rate. Naked samples were suspended in the TGA with platinum wire (instead of the pan) allowing more intimate contact between the sample and the oxidizing gas flow. Five NBG-25 buttons from the same source stock were also tested in the INL vertical furnace at three temperatures. Only one of the five was tested at the nominal 650°C temperature, but two each were tested at 700°C and at 750°C. Neither of the two tested at 750°C showed the type of grain loss observed in the large samples. For the five naked NBG-25 button samples tested in the TGA using the 150 mL/min flow rate, performance in the TGA and the vertical furnace seems to be comparable (Figure 5). This is an important conclusion resulting from this careful comparison of oxidation behavior. It may explain contradictory results observed between different laboratories conducting similar oxidation-rate studies on the same graphite grade. It demonstrates that any oxidation test conducted outside the standardized ASTM D7542 conditions *must* be verified to supply excess oxygen (at the graphite surface) before the results can be compared to other oxidation studies.

The use of a closed-bottom pan appears to influence the graphite-oxygen interface significantly: as shown in Figure 5; more rapid oxidation was observed for the sample oxidized naked in the TGA at the same 150 mL/min, 700°C conditions as the sample oxidized in the TGA pan. Hereafter, the term basket will be reserved for an open platinum-wire construct as employed in the vertical furnace, and TGA samples will be described as either suspended naked or in pan. Consistent use of open-weave thin wire constructs to immerse the sample fully within the gas flow allows more uniform exposure to excess oxygen.

One additional NBG-25 button was available and was tested in the TGA at the highest temperature with a flow rate of 200 mL/min, approaching the reaction rate observed in the vertical furnace even more closely. The relatively small change in the observed oxidation rate rising from 150 to 200 mL/min also seems to be consistent with the aforementioned diminishing influence of increasing gas flow. At up to ten percent mass loss, there was no evidence of gross grain loss from any of the buttons tested in either the TGA or vertical furnace system.

A comparison of the linearity of Arrhenius relationships, even with these limited data sets (five points each), suggests that the naked samples tested in the TGA with 150 mL/min air flow were oxidizing within the same regime ( $R^2 = 0.999$ ), while observed performance of samples of the same grade tested in the vertical furnace were somewhat mixed ( $R^2 = 0.978$ ). Even without indications of grain/particle loss (diffusion effects at the sample surface) observed in larger samples, scatter in the vertical-furnace data belies the statistical limitations of the larger-scale equipment. The TGA is a precision instrument for mass measurement at controlled temperature, and physical limitations of the less precise vertical-furnace system introduce compounding inaccuracies (between runs and even more so between operating campaigns, where the system is disassembled and reassembled). The TGA chamber provides a uniform reaction environment compared to which the vertical furnace gives only a crude approximation.

### 2.5.3 Sample Size and Fundamental Differences in Length Scale

In theory, similar environmental test conditions should produce a similar reaction rate in the same material. However, one obvious distinction between graphite oxidation in the TGA as compared to the vertical furnace is that TGA-specimen dimensions are much smaller and proportioned differently from materials tested in vertical-furnace systems. Sample size (fundamental differences in length scale) can produce notable variations, as exemplified by the variation in oxidation rate with extent of reaction, illustrated by the shape of the onset curve as shown in Figure 6. Note that the onset curve for a button sample is distinctly different from the onset curve for a larger sample, even when other test conditions are duplicated in the same vertical furnace. However, in this case, the slope of the nominally linear five to ten percent mass-loss portions of these curves match relatively well.

Note that deviations in local conditions produce observable discrepancies in the overall reaction rate with different length scales. Recognized as an artifact of onset for a partially oxidized body of graphite material, this is understood loosely as the effective pore evolution.

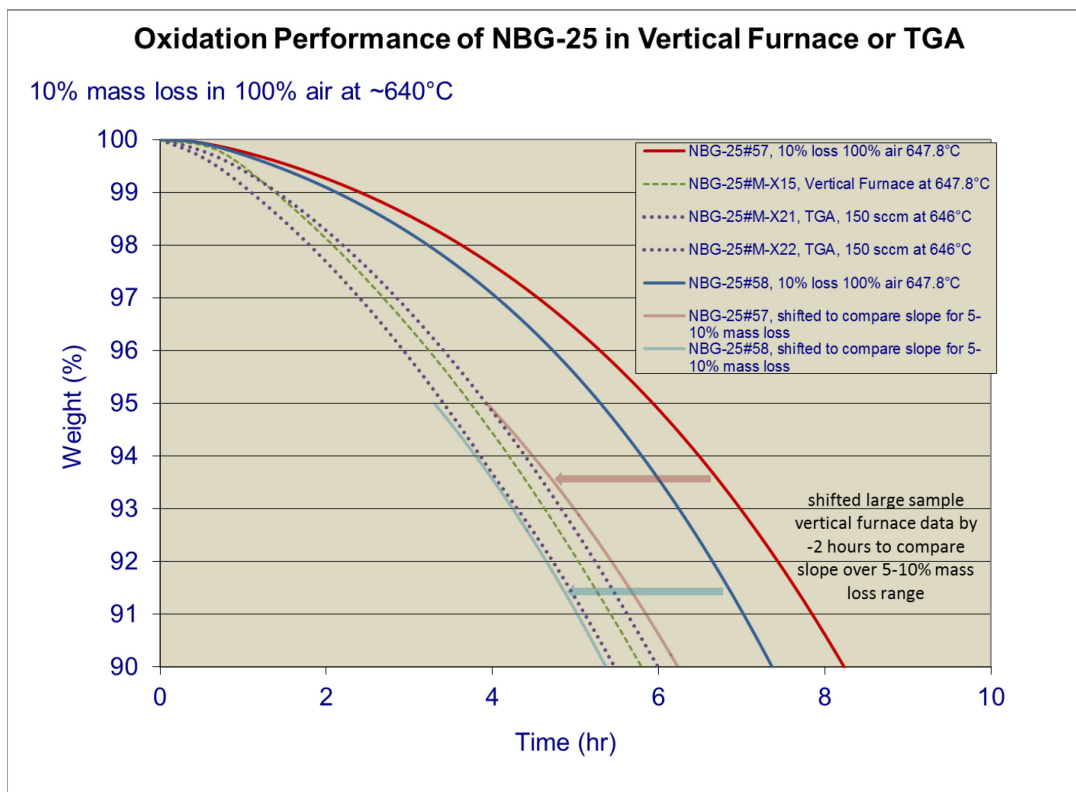


Figure 6. Sample geometry alters onset while approaching same linear oxidation rate.

### 3. MATERIALS AND METHODS

The premise of this experiment was to assess TGA operating conditions for two extremely different grades of graphite to determine whether parallel results could be achieved to match vertical furnace results under isothermal oxidation conditions comparable to those established in ASTM D7542. The preliminary work with NBG-25 suggested that gas-flow rates of 150 mL/min or higher could provide suitable TGA conditions to match the vertical furnace results (with an oxidizing gas flow of 10 L/min air) over substantially the same test temperatures as long as the samples were suspended naked for full immersion in the oxidizing gas flow. To assist in determining the appropriate testing conditions, an additional scoping study was conducted to establish the gas-flow rate to be used in the TGA.

TGA oxidation rates for the NBG-25 graphite tested at 150 mL/min gas flow are slightly lower than those from the vertical furnace. Therefore, gas-flow rates of 150, 180, and 200 mL/min were tested at 680°C in the TGA using the fine-grain, isostatically molded IG-110 material. The slightly lower temperature was used to avoid complications from surface effects because vertical-furnace testing of the larger IG-110 samples suggested that IG-110 could be susceptible to loss of grains/particles and indications of marginally sufficient oxygen at temperatures as low as 700°C.

Three samples were tested at each of the three gas-flow rates at a consistent 680°C set point. Ignoring the flow effects (on the assumption that all three variations supply an excess of oxygen), the average oxidation rate across all nine samples was  $111.82 \text{ g h}^{-1} \text{ m}^{-2}$  ( $1.0963 \times 10^{-5} \text{ g s}^{-1} \text{ g}_0^{-1}$ ) with the standard deviation being  $6.33 \text{ g h}^{-1} \text{ m}^{-2}$  ( $6.22 \times 10^{-7} \text{ g s}^{-1} \text{ g}_0^{-1}$ ). The details are given in Table 2 and Figure 7. As these data show, variations in tests repeated under identical conditions are large compared to the observed and diminishing trend of increasing oxidation rate with increasing air-flow rate. From these results, interpreted in the context of the preliminary data in Table 1, further increases in air flow rate were inferred to have relatively little additional effect on the observed reaction rate, and a set point of 200 mL/min was adopted for the TGA.

Table 2. Naked IG-110 samples tested at 680°C to determine TGA air flow rate for oxidation testing.

Sample ID	Air Flow Rate (mL/min)	Surface Area Normalized Oxidation Rate (g h <sup>-1</sup> m <sup>-2</sup> )	Average Surface Area Normalized Oxidation Rate (g h <sup>-1</sup> m <sup>-2</sup> )	Mass Normalized Oxidation Rate (g s <sup>-1</sup> g <sub>0</sub> <sup>-1</sup> )	Average Mass Normalized Oxidation Rate (g s <sup>-1</sup> g <sub>0</sub> <sup>-1</sup> )
#18	150	102.72	105.53 ± 4.52	1.0052E-05	1.0328E-05 ± 4.499E-07
#20		110.74		1.0847E-05	
#23		103.13		1.0085E-05	
#22	180	107.40	114.35 ± 6.02	1.0553E-05	1.1232E-05 ± 5.886E-07
#30		117.85		1.1546E-05	
#31		117.81		1.1597E-05	
#32	200	119.04	115.59 ± 3.65	1.1622E-05	1.1330E-05 ± 2.933E-07
#33		115.97		1.1331E-05	
#34		111.76		1.1036E-05	
Overall Average without Regard for Flow Effects		111.82 ± 6.33		1.0963E-05 ± 6.224E-07	

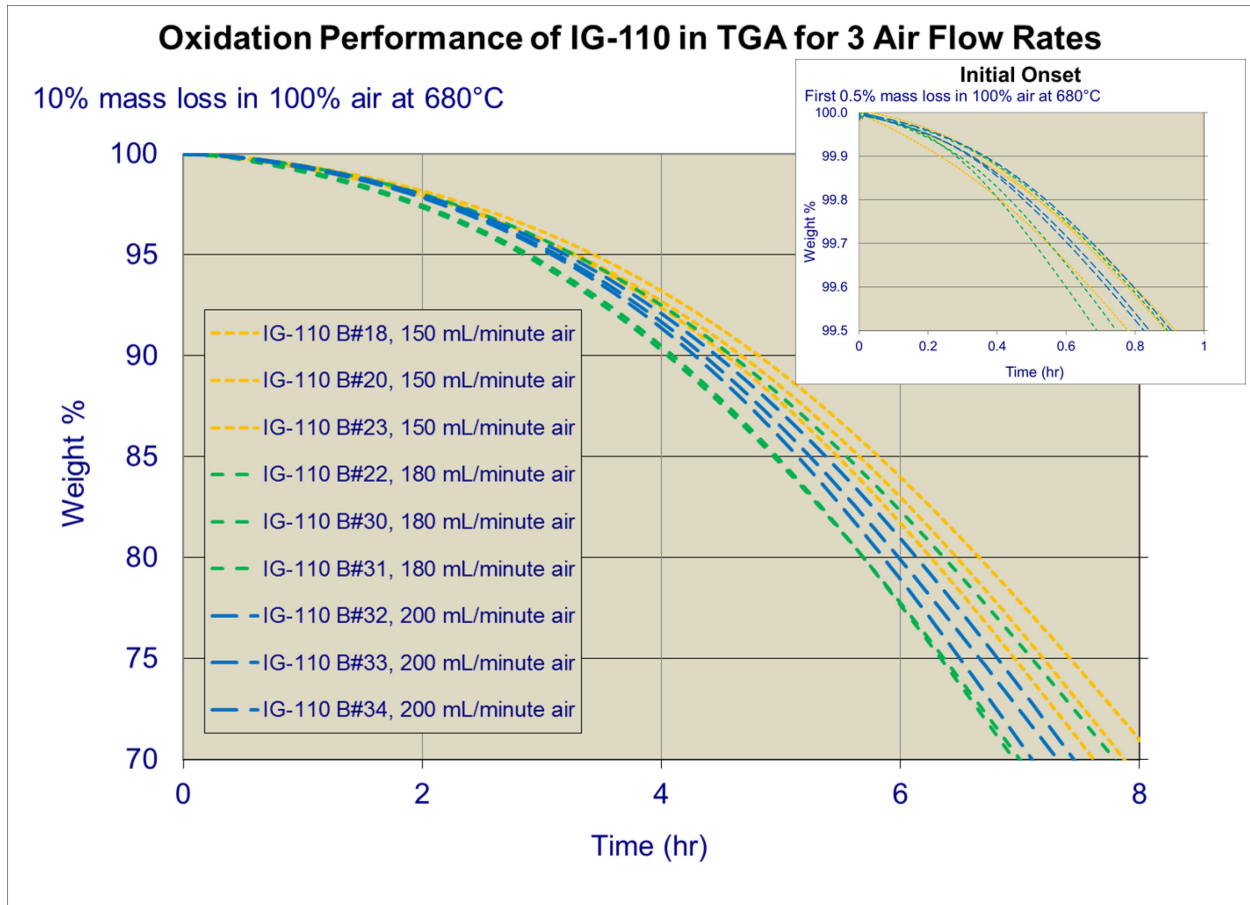


Figure 7. Variations in onset for three TGA flow rates over the first 0.5% mass loss and up to 30% mass loss.

In Figure 6, where only ten percent mass loss is shown, the 95 to 90% weight range of interest appears to be quite straight. Objectively, this part of the curve is nearly linear, with an R-squared value between 0.996 and 0.999 for each of the five mass-loss curves shown. Figure 7 shows more of the mass-loss curve for TGA data, down to ~30% mass loss for nine button samples tested. The TGA mass-loss curves in Figure 7 are similarly straight (based on the correlation coefficients) over the same 95 to 90% weight range, but qualitatively, the curvature of the aggregate data is apparent. The slope of the 95 to 90% segment is noticeably less steep than the 80 to 75% segment for each of the curves shown. The use of the 95 to 90% segment is reasonable for expedience and will always be quite conservative by comparison to the first five percent of mass loss.

However, these data show both the somewhat arbitrary nature of the concept of onset and that slightly faster oxidation may occur after ten percent mass loss and before the rate slows at the tail of the mass-loss curve, depending on the graphite dimensions and oxidation conditions. Also, small segments of the mass-loss curve (representing  $\leq 5\%$  weight change) are likely to be nearly linear under most conditions beyond the first few percent mass loss (unless entire grains of filler material drop off the sample surface). Zooming in on the first 0.5% of mass loss, note that there is no appreciable difference in onset with gas-flow rate over the first hour of oxidation.

### 3.1 Basic Test Plan (and Its Basis)

Three sets of experiments were conducted for two grades of graphite. Button samples and larger compression-test samples were cut from the same source slabs of IG-110 and NBG-18 graphite. Button

samples were to be tested in the TGA and in the vertical furnace at a suite of temperatures between 560 and 740°C. Larger compression-test samples were also to be tested in the vertical furnace under a parallel set of environmental conditions. Three replications were planned for each set of conditions to provide additional insight into statistically meaningful variations in the data.

### 3.2 Selection of Sample Materials

These two grades were selected to represent a wide range of nuclear graphite materials. IG-110 has a fine-grained petroleum-coke filler with petroleum-coke binder, while NBG-18 has both a relatively large average grain diameter and a wider distribution of pitch-coke filler particle sizes with a coal-coke binder. Prior work suggested the medium grained NBG-18 is one of the more oxidation-resistant graphite grades. By contrast, the fine-grained IG-110 appears more vulnerable to oxidation; it is subject to gross loss of surface material where other grades exhibit slower mass loss, distributed more uniformly through the sample, for the same test conditions. The NBG-25 used in the scoping trial is similar to IG-110, both in comparatively fine grain size and in petroleum-coke origin.

### 3.3 ASTM Protocol as Adapted for Use

With the exception of sample dimensions, vertical-furnace operation is derived directly from the ASTM D7542 standard. Graphite oxidation test protocol includes the following environmental controls.

12. Temperature is maintained within  $\pm 2^\circ\text{C}$  of the set point (as measured near the sample) for at least 1 hour before the start of and throughout oxidation. The TGA chamber provides much tighter temperature control than does the vertical furnace. The TGA vessel has a more uniform hot zone, and the measured temperature seldom drifts more than a couple tenths of a degree. The vertical furnace controller is optimized for operation at a nominal 700°C, it takes much longer to stabilize at temperature than does the TGA, and it does not maintain low temperatures reliably (i.e., below 600°C, there is significant risk that the furnace never achieves the requisite  $\pm 2^\circ\text{C}$  of the set point over a 60-minute period). However, in both cases an isothermal period before the transition to air provides a pre-oxidation validation of mass as measured in flowing gas at temperature.
13. Oxidation tests are concluded after a specified minimum mass loss is achieved; for the purpose of determining kinetic parameters for a graphite material, at least ten percent mass loss is preferred. The vertical furnace control is fully automated allowing cool down in inert gas for controlled sample recovery.
14. Total gas flow is maintained at 10 L/min throughout each vertical furnace test, employing bottled nitrogen during system-warmup phase and house instrument air (during oxidation phase), each flowed through a moisture trap with integral molecular sieve.
  - TGA operation employs similarly conditioned gases flowed at 200 mL/min through the reaction chamber, as determined from the evaluation of data presented in Table 2. Throughout both the scoping work and the main experiment, the TGA employed a helium purge rate of 30 mL/min to the instrument cavity. The TGA runs a timed sequence and requires operator intervention for shutdown based on specific mass loss. TGA cooldown is in air, so samples are not suited for controlled post-oxidation testing (although the TGA cools from isothermal set point to a nominal 50°C in about half an hour, compared to over 14 hours for the vertical furnace to cool from the same set point). Generally, any TGA data for oxidation beyond ten percent mass loss is simply disregarded.
15. Button dimensions are within TGA-capacity limitations and generally conform to ongoing graphite irradiation specimens for future experimental applications of interest. The compression-test sample diameter meets the cross-sectional dimension in the oxidation standard, but the sample height is doubled from what is specified in ASTM D7542 to match the compressive-strength test standard, ASTM C695.

16. In both the TGA and the vertical furnace (for the sample sizes of the articles tested), oxidation onset appears to have progressed sufficiently so that the reaction rate is satisfactorily linear for the five to ten percent mass-loss range. This reaction rate is used for the evaluation of kinetic parameters as indicated in consensus standard ASTM D7542. However, when considering samples of different and disproportionate geometries, as button and compression samples are, choice of normalization matters.

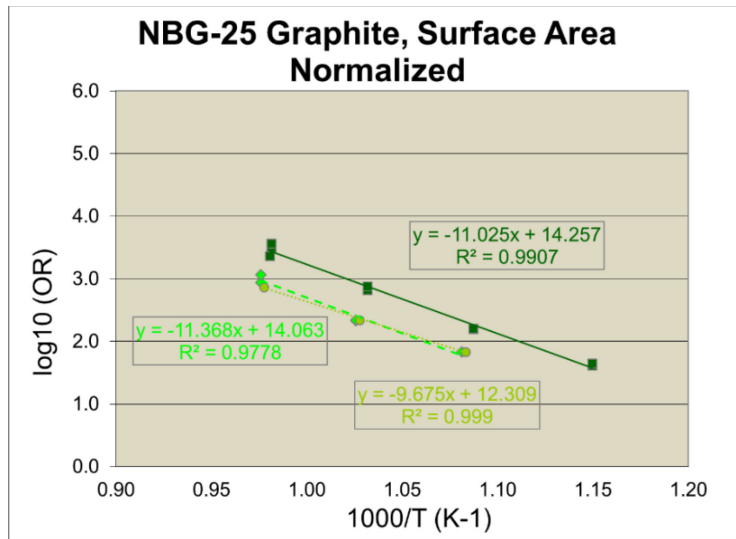
### 3.4 Normalization of Data

The ASTM D7542 presents two conventions for data normalization: normalize the resultant rate data by the initial geometric surface area of the graphite sample, or normalize the resultant rate data by the initial mass of the graphite sample. Surface area normalization may be preferred if all of the samples of interest are of the same nominal dimensions. However, if the interest is in comparing performance across samples of varying sizes or shapes, mass normalization provides a more useful format. While the extremes of Figure 1 (bottom) suggest a dramatically more rapid oxidation of a long thin sample by comparison to a short fat sample of the same nominal mass, observed variations can be minimized by normalizing by mass rather than by surface area. For testing under ASTM D7542 that seeks to emphasize observable differences in performance among grades of graphite, surface area normalization is appropriate. However, in the interest of comparing across different systems, specifically with varying length scales, mass-normalized data provide a more convenient tool for comparison.

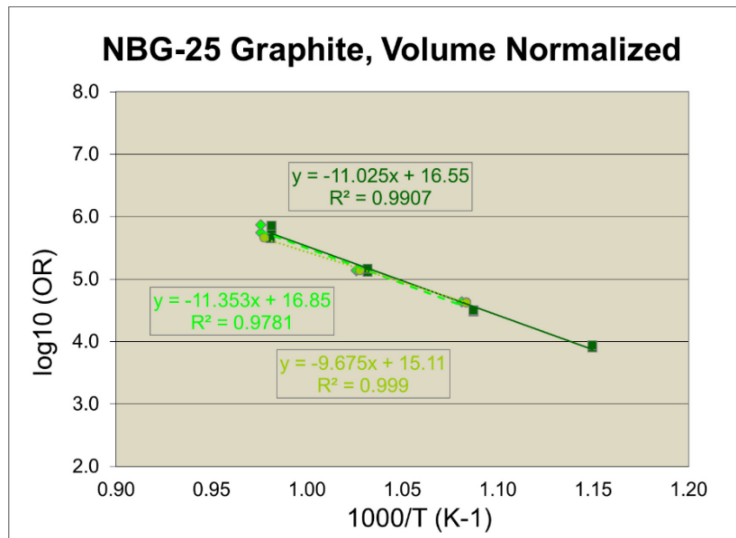
Kim, Lee, and No<sup>6</sup> demonstrated favorable results in their comparison of IG-110 data for numerous specimens tested at 600°C in a controlled, dry air flow in a vertical furnace. Their analysis specifically varied the surface-area-to-volume ratio without giving mass data explicitly. Their work considers an internal surface area proportional to sample volume, which correlates to volume normalization. However, using the highly uniform density of virgin IG-110 graphite (1.75 g/cm<sup>3</sup>), their data can be shown to give excellent agreement when converted to a mass-normalized basis.

Results from the NBG-25 scoping trial (shown in Figure 5 and Table 1) are illustrated in Figure 8 (excluding those TGA samples that were suspended in the pan), with data normalized by initial volume, by initial geometric surface area, and by initial mass. Again, the highly uniform density of the virgin NBG-25 graphite provides for similar convergence with both volume- and mass-normalization methodologies. Given the apparent increase in scatter in data evident at the highest temperature tested, the crucial consideration for the convergence of the mass and volume normalized data appears to be the availability of excess oxygen achieved with sufficiently high gas flow. Note that these data, in conjunction with the IG-110 data given in Kim, Lee, and No,<sup>6</sup> further substantiate the choice of the 200 mL/min air-flow rate and the selection of more moderate temperatures for this study.

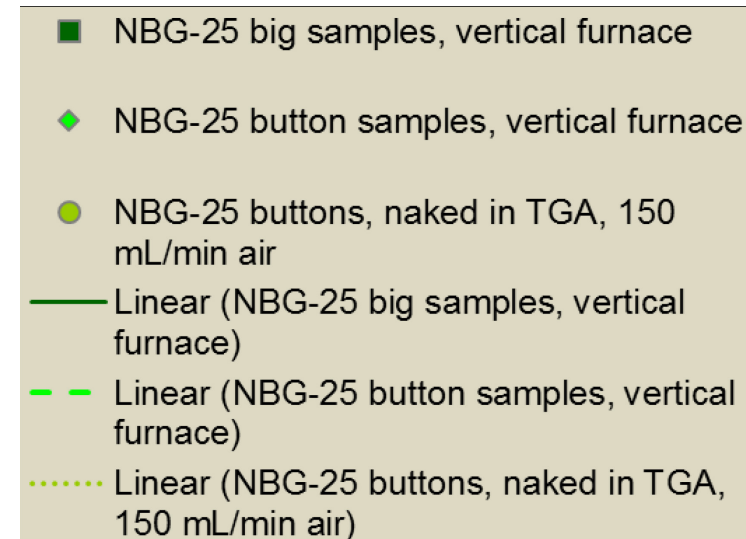
Disparities in surface-area-to-volume ratios with TGA and vertical-furnace samples obscure comparison among systems unless data are mass- or volume-normalized. Mass is simpler to measure with accuracy than volume and surface area and, therefore, is preferred even though volume normalization might be advantageous in discerning performance differences with variations within graphite grade. The preliminary data illustrated in Figure 6 and Figure 8 support the premise that mass-normalized reaction rates allow comparison (over the same temperature range) regardless of system or sample geometry (once the nearly linear reaction rate is established) as long as a suitable excess of oxygen is available in all cases.



(a)



(b)



(c)

Figure 8. NBG-25 graphite oxidation Arrhenius data: (a) surface area normalized and (b) volume normalized, and (c) mass normalized.



## 4. RESULTS AND ANALYSIS

This effort produced two families of self-consistent Arrhenius data, as plotted in Figure 9.

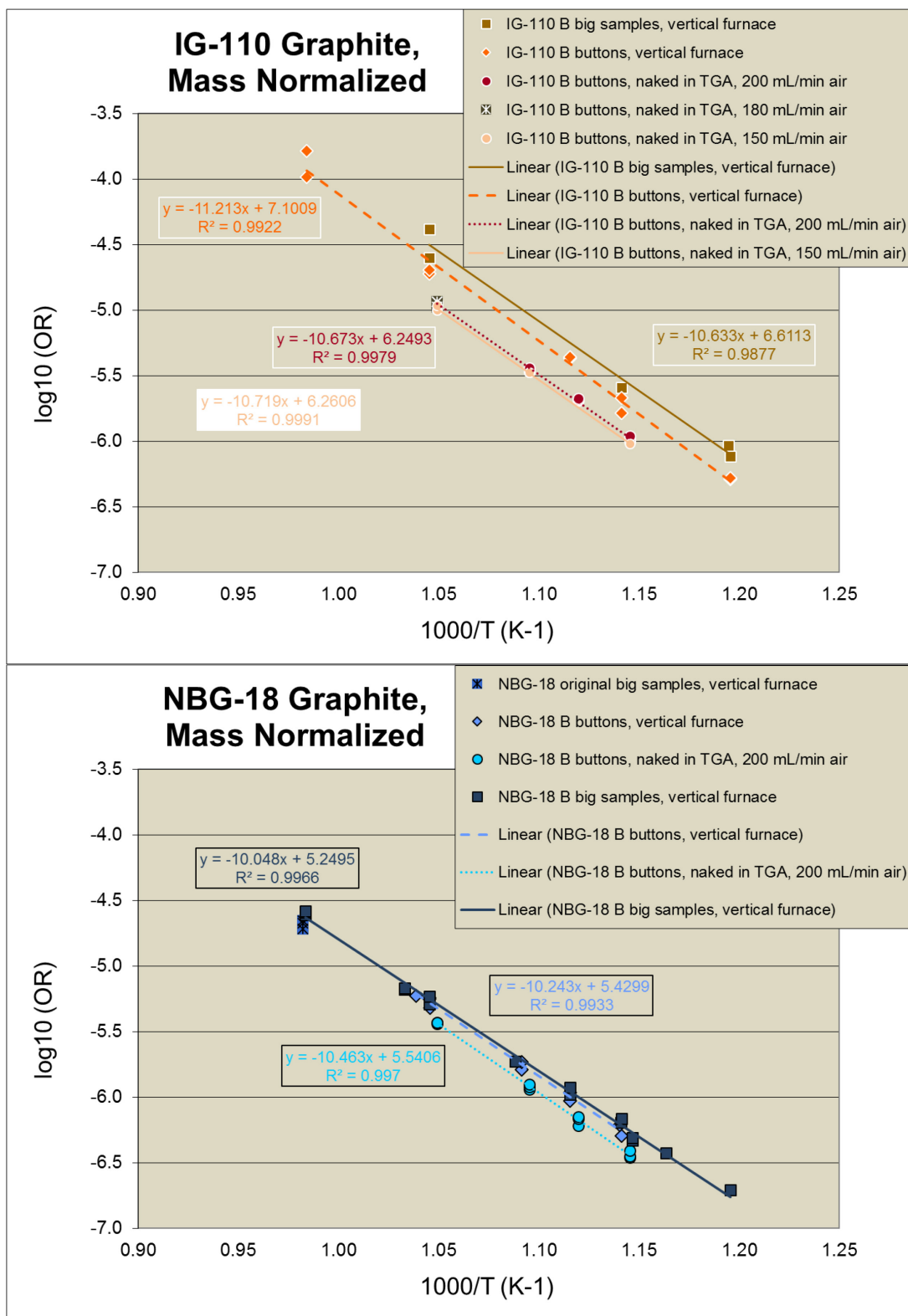


Figure 9. Self-consistent families of data for IG-110 (top) and for NBG-18 (bottom).



All TGA runs used the same thermocouple, naked suspension configuration, and 200 mL/minute air flow; all vertical-furnace runs were performed between the same two calibration dates, with the same thermocouple and sample suspension configuration, and 10 L/minute air flow. Notably, these data for IG-110 and NBG-18 do not superimpose quite as neatly as the NBG-25 appeared to in Figure 8(c), possibly because of thermocouple variations. However, considering the amount of scatter generally present in the vertical-furnace data, the similarity in slope does give good agreement in the derived activation energy for each graphite grade.

Considering the two families together on the same axis in Figure 10 suggests that the IG-110 performance may be influenced more by both geometry and gas-flow parameters. However, the relative performance indicating NBG-18 to be more resistant to oxidation than IG-110 is consistent.

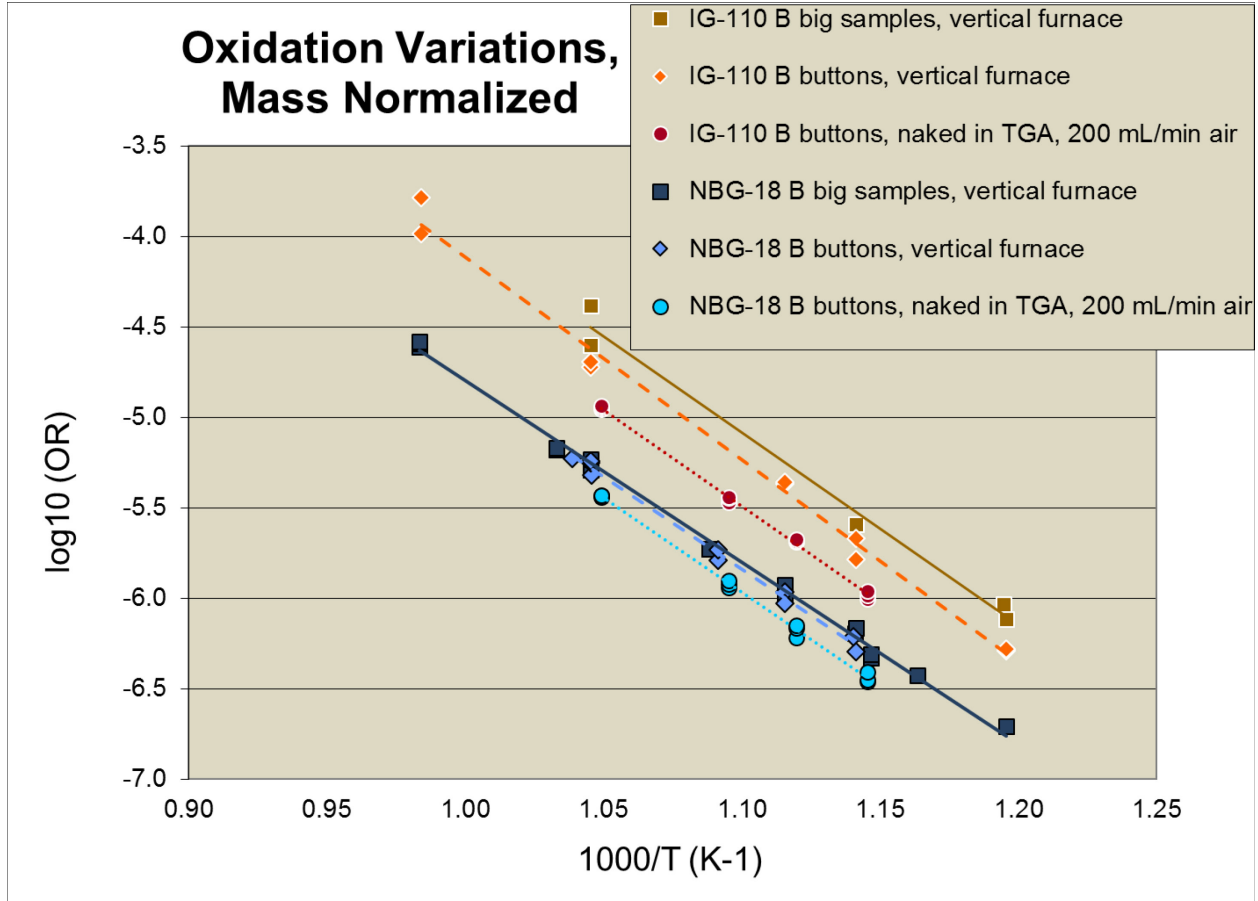


Figure 10. Mass-normalized oxidation rates for IG-110 and NBG-18 in the TGA (buttons) and in the vertical furnace (buttons and big samples).

Comparing the two sample geometries tested in the vertical furnace first, the NBG-18 data nearly converge for the button and big samples. However, the disparate sample dimensions seem to have a more pronounced effect for the IG-110 graphite. Looking next to the button samples, comparing the TGA data to the vertical-furnace data for the same nominal sample dimensions, NBG-18 shows a distinct offset. However, IG-110 data show an even larger offset comparing oxidation performance between the TGA and the vertical furnace. In all cases, the NBG-18 is shown to be more resistant to oxidation than the IG-110. These data confirm that both the air-flow conditions and the sample geometry affect the extent to which diffusion influences the observed oxidation rate. Over the range of temperatures tested, both diffusion and geometry effects are much more pronounced for the IG-110 material than for the NBG-18 material.

Those initial observations from NBG-25 oxidation presented in Figure 8 in actuality reflect a combination of multiple effects. The NBG-25 data collected in the TGA reflect oxidation at the lower air-flow rate of 150 mL/minute. The limited number of temperatures and the small button-sample geometry tested in the TGA obscured evidence of diffusion effects at the temperatures employed. The three preliminary NBG-25 data sets reflect some of the shortcomings of fortuitously collected data.

Vertical-furnace data over the same nominal temperature range, but with the substantially higher (linear and volumetric) air-flow rate, show a significant difference in slope, as plotted alongside the TGA data. The vertical-furnace data may be more nearly indicative of the chemical kinetics: the diffusion influences in the vertical furnace data were mitigated by both the higher air flow and (for the big samples) by additional data available from a greater number of lower-temperature runs. Perhaps a TGA gas-flow rate of 150 mL/minute is starving the NBG-25 reaction for oxygen: at temperatures of 750 and 700°C; a higher air-flow rate would produce a consistent, if small, increase in observed oxidation rate in agreement with the observations for IG-110 given in Table 2. This effect can be seen directly for the single 200 mL/minute NBG-25 datum included on the plot in Figure 5. Limited NBG-25 sample availability inhibited conducting a more thorough investigation of TGA air flow rates at the time.

In hindsight, the NBG-25 data suffer from three potentially significant functional inconsistencies. First, the big samples are not traceable to the same source billet as the button samples. Second, due to the installation of the TGA in a radiological area, the TGA thermocouple in use at the time of the NBG-25 testing had not been calibrated. It was spot-checked against a calibrated thermocouple in a nearby furnace and was found to read approximately 4°C above the improvised reference at 700°C. And third, the thermocouples in the vertical furnace came due for calibration after the NBG-25 big samples had been tested and were removed, calibrated, and reinstalled before the NBG-25 button samples were tested.

All three of these variables were controlled, to the fullest extent possible, for IG-110 and NBG-18 testing. First, both the big IG-110 samples and the IG-110 button samples were cut (with the same grain orientation) from a single slab, designated IG-110 B. Likewise, the NBG-18 big and button samples were also cut from a single slab, designated NBG-18 B. Second, the TGA thermocouple is now routinely calibrated in accordance with INL Quality Assurance procedures. Third, all data shown in Figure 10 were collected without any disassembly or configuration changes during the experiment campaign interval. In fact, an earlier subset of NBG-18 big samples was tested with the same thermocouples, but the data were excluded from Figure 10 because the disassembly and reassembly of the vertical furnace necessary for calibration can cause a slight shift in performance (on the same order as the typical scatter in vertical furnace data).

## 5. CONCLUSIONS

The initial hypothesis that, for a judiciously selected gas flow rate, TGA performance would match the oxidation performance observed in the vertical furnace only partially holds true. When the mass-normalized oxidation rate matches in the two systems with dissimilar sample geometries, the high-temperature performance may depart from the “linear Arrhenius plot” at significantly different temperatures. The match is best at lower temperatures and for more robust grades of material. For materials more susceptible to surface effects (for example, gross grain loss) the mass-normalized button and big samples oxidized in the vertical furnace do not match each other or their companion TGA data quite as well. This is in keeping with the traditional theory of a low-temperature “kinetic regime” (Regime 1). However, the sample geometry and the air-flow rate influence the observed “transition” (bend in the Arrhenius plot), with results that are not entirely consistent across disparate graphite grades. The bend in the Arrhenius plot may occur at a different (lower) temperature in the TGA than for samples of the same material tested in the vertical furnace, even as the bend occurs at different temperatures, depending on the air flow or the grade of graphite (tested in the same equipment). Fundamentally, the gas flow in the TGA was limited (to 200 mL/min) by the available control system.

These data substantiate that comparison of rate data between TGA and vertical furnace results can be made for some well-defined conditions, but only in the context of consistent control. Substantial differences in sample dimensions and in geometric proportions can be somewhat compensated with mass normalization, as long as diffusion effects are small relative to the chemical kinetics (i.e., air flow is sufficiently high). Because variations in gas flow and variations in sample geometry can influence oxygen availability, presence of excess oxygen must be confirmed to validate the range of conditions over which the data from disparate systems can be compared. Statistical reproduction of testing over a suitable range of parameters appears to be more important than accommodating larger specimens, which necessarily limits the test matrix for irradiated materials.

In order to build a significant body of oxidation data from multiple research studies, all graphite oxidation testing must quantify the oxidation rate as a material-specific property by tightly controlling the test conditions so that intrinsic material-specific factors will govern the observed results. However, as this study demonstrates, graphite oxidation behavior is affected, to a greater or lesser extent, by a wide range of test-parameter variations other than just graphite grade and oxidation temperature. Additionally, practical constraints crucial for relating the observed oxidation of small test specimens to the oxidation behavior of larger, standardized test samples must be considered along with conditions keeping the tests focused on the intrinsic response. The major test parameters, or conclusions, identified from this study are listed to highlight these experience derived insights into graphite oxidation testing.

17. Any oxidation test conducted outside the parameters established within a standardized test method (i.e., ASTM D7542) must be verified to supply excess oxygen (at the graphite surface) before the results can be compared to other oxidation results.
18. A test environment with surplus oxygen (an unvarying  $P_{O_2}^n$  term across the entire temperature range) completely surrounding the graphite test specimen is critical:
  - c. Before data from different oxidizing apparatus can be compared (i.e., vertical furnace versus TGA), the flow rate of the oxidizing gases must be established. Suitable gas flows—considering internal chamber diameter, specimen size, specimen geometry, and system capabilities—must be established to ensure surplus oxygen during testing.
  - d. For a direct comparison of TGA and vertical-furnace results (small specimens versus large specimen) excess oxidizing gas must be present for the full range of temperature test conditions. This will produce the same linear oxidation rate when averaged over the sample mass.
19. Theoretical graphite oxidation is traditionally conceived as three distinct temperature-dependent regimes. However, empirical rate data show a continuum response, where actual physical conditions at the extremes are theoretical approximations. A more meaningful model blends the characteristics of diffusion and chemical kinetics across the entire spectrum of observable performance.
  - c. From a practical perspective, low-temperature oxidation is very slow, and maintaining controlled experiment conditions for long periods is problematic. Also, at low temperatures, the anticipated flat concentration profile is still only approached for small and/or thin graphite specimens.
  - d. Alternately, high-temperature oxidation of small specimens is so rapid that the air-flow rate becomes reaction limiting, and real-time mass loss measurement becomes difficult.
20. While the observed oxidation response is a continuum, the **effect of oxidation** on the actual graphite material is dramatically different even across a limited span of experimental test temperatures (nominally 550 to 800°C):
  - d. At high temperatures, graphite oxidizes only on the surface of the specimens and occurs as fast as oxygen can be transported to the surface of the sample; this is known as the “shrinking core” model of graphite oxidation. Little to no oxygen penetrates into the interior microstructure.

*Because only the outer surface is affected, mechanical-strength loss is minimized at highest temperature when compared to low-temperature oxidation.*

- e. At low temperatures, graphite oxidizes uniformly throughout the entire penetrated volume. The extent of oxidation in the sample interior will be nearly the same as the exterior surface. *Because of the internal damage, mechanical-strength loss is maximized when compared to high-temperature oxidation.*
  - f. All intermediate temperatures will produce a gradient of partial oxidation, with the penetration depth dependent upon the unique grade microstructure and test temperature.
21. Oxidation mass-loss progression falls into three distinct developmental periods:
- d. *Onset*: The initial period is concomitant with the dynamic evolution of internal porosity. This is denoted as the non-linear, initial portion of the mass-loss to time curve before a stable rate of mass loss is achieved. It is conventionally defined as mass loss from 0–5%, and it can take up to 15% mass loss before the internal pore structure is fully established.
  - e. *Pseudo-steady-state*: This period corresponds to the stable relationship between gas gradients, graphite density gradient, and a consistent concentration of active sites (on average) sustained after onset. It is denoted as the nearly linear portion of the sigmoidal mass-loss-to-time curve. Conventionally, it is measured as mass loss from five to ten percent, but it more accurately occurs between 15 and 25% mass loss, after onset and before the pore microstructure is affected by significant mass loss.
  - f. *Tail*: The period at the end of oxidation, after significant mass loss has occurred, is when the asymptotic non-linear segment of the mass-loss curve reflects the approximate inverse of onset, where rate deceleration accompanies the declining concentration of active sites (on average across the sample, local porosity allows for ample gas exchange, but less and less graphite is locally present to react).
22. Impurities within the (carbon) graphite material can significantly alter the oxidation rate and behavior. Contaminants may catalyze or inhibit oxidation (or neither), and the tail may exhibit the increasing influence of impurities as the ash residue represents progressively more of the remaining mass.
23. Tests with fine-grain grades are more susceptible to an issue with small grains or particles separating from the surface of the specimen. This can produce artificially high measured oxidation rates.
24. Sample size (fundamental differences in length scale) can produce notable variations, as exemplified by the variation in oxidation rate with extent of reaction. *Sample dimensions should be consistent to provide some control of onset variations.*
25. The depth of oxidation penetration into the sample interior is interdependent to the density gradient caused by the progression of oxidative mass loss.
26. Masking the contact surface of the sample from the impinging gas flow must be avoided. *The use of a closed bottom pan within a TGA system appears to influence the graphite-oxygen interface significantly.*
27. Choose the correct normalization method for oxidation data.
- c. For testing under ASTM D7542 that seeks to emphasize observable differences in performance *among grades of graphite*, surface area normalization is appropriate.
  - d. However, in the interest of *comparing across different oxidizing systems*, specifically with varying length scales, mass-normalized data provide a more convenient tool for comparison.

These conclusions summarize the observations that most impact oxidation behavior under experimental test conditions and provide the fundamental principles for comparison of test results from disparate experimental systems. Given the limited availability of irradiated graphite for oxidation test material, these principles are essential for developing meaningful experimental results relevant to nuclear reactor graphite applications.

## 6. REFERENCES

1. J. J. Kane, C. I. Contescu, R. E. Smith, G. Strydom, and W. E. Windes, "Understanding the reaction of nuclear graphite with molecular oxygen: Kinetics, transport, and structural evolution," *Journal of Nuclear Materials* Vol. 493 (2017), pp. 343–367.
2. P. L. Walker, Jr., F. Rusinko, and L. G. Austin, "Gas Reactions of Carbon," *Advances in Catalysis* Vol. 11 (1958), pp. 133–221.
3. A. C. Matthews, J. J. Kane, W. D. Swank, and W. E. Windes, *The Degradation of Strength under Varying Oxidizing Conditions for Nuclear Graphite*, INL/EXT-19-53723, April 2019.
4. R. P. Wichner, T. D. Burchell, and C. I. Contescu, "Penetration depth and transient oxidation of graphite by oxygen and water vapor," *Journal of Nuclear Materials* Vol. 393 (2009), pp. 518–521.
5. C. I. Contescu, S. Azad, D. Miller, M. J. Lance, F. S. Baker, and T. D. Burchell, "Practical aspects for characterizing air oxidation of graphite," *Journal of Nuclear Materials* Vol. 381 (2008), pp. 15–24.
6. Eung Soo Kim, Kyung Won Lee, and Hee Cheon No, "Analysis of geometrical effects on graphite oxidation through measurement of internal surface area," *Journal of Nuclear Materials* Vol. 348 (2006), pp. 174–180.